Synthesis and Characterization of in Situ Cross-Linkable Hyaluronic Acid-Based Hydrogels with Potential Application for Vocal Fold Regeneration

Xinqiao Jia,[†] Jason A. Burdick,[†] James Kobler,[‡] Rodney J. Clifton,[§] John J. Rosowski,[⊥] Steven M. Zeitels,[#] and Robert Langer*[,†]

Department of Chemical Engineering, Massachusetts Institute of Technology, 77 Massachusetts Ave., E25/342, Cambridge, Massachusetts 02139; H. P. Mosher Laryngological Research Laboratory, Massachusetts Eye and Ear Infirmary, Boston, Massachusetts 02114; Division of Engineering, Box D, Brown University, Providence, Rhode Island 02912; Eaton-Peabody Laboratory, Massachusetts Eye and Ear Infirmary, Boston, Massachusetts 02114; and Department of Otology & Laryngology, Harvard Medical School, Division of Laryngology, Massachusetts Eye and Ear Infirmary, 243 Charles St., Boston, Massachusetts 02114

Received December 21, 2003; Revised Manuscript Received February 18, 2004

ABSTRACT: Despite a well-recognized clinical need for a material to replace missing or damaged vibratory connective tissue of the vocal fold, materials have yet to be engineered specifically for this purpose. Injectable hydrogels are particularly attractive because they would require a minimally invasive surgical procedure, could fill irregular defects, and could be designed to have viscoelastic properties similar to the normal tissue. We therefore synthesized a series of photo-cross-linkable hydrogels using hyaluronic acid (HA) as the starting material. The hydrogel precursors studied included HA modified with glycidyl methacrylate (HA/GMA), HA partially oxidized by sodium periodate (HAox) followed by GMA conjugation (HAox/GMA), and HA grafted with a synthetic polymer before introduction of GMA. The synthetic polymer employed was oligomeric poly(2-hydroxyethyl methacrylate) (P(HEMA)) with 31 mol % poly(*N*,*N*-dimethylacrylamide) (P(DMAM)), and the resulting hydrogel precursors were referred to as (HAox-*g*-P_y)/GMA (*y*%: grafting percent). The macromonomers were characterized by GPC and ^{1}H NMR. Hydrogels were obtained by subjecting the aqueous macromonomer solutions to UV irradiation in the presence of a photoinitiator. Under physiological conditions HAox/GMA hydrogel exhibited the highest swelling ratio and degraded most readily, whereas (HAox-*g*-$P_{1.9}$)/GMA hydrogel swelled to a lesser extent and was most resistant to enzymatic degradation. Mechanical tests using an acoustic shaker yielded viscoelastic properties from 20 to 180 Hz. HAox/GMA hydrogel showed the lowest viscoelastic modulus and viscosity while (HAox-*g*-$P_{1.9}$)/GMA hydrogel exhibited the highest values. The interior structures of the fully swollen hydrogels examined by scanning electron microscopy (SEM) showed the presence of fibrous or porous morphology. The cell cytotoxicity study indicated that HAox/GMA macromonomer was cytocompatible at concentrations less than 0.2 mg/mL, and there was no loss of cells when encapsulated in (HAox-*g*-$P_{1.9}$)/GMA photo-cross-linked network. These new hydrogels have potential as injectable formulations for regeneration of the vocal fold's mucosal layered microstructure.

Introduction

Vocal fold vibration depends critically on the viscoelasticity of the connective tissue of the vocal fold mucosa. The presence of scar tissue reduces the natural pliability of the lamina propria, causing hoarseness and other symptoms of vocal dysfunction. An estimated 5−10% of the population is affected by some degree of vocal fold scarring. Scar tissue within the superficial layers of the vocal fold can be removed using microsurgical techniques;[1,2] however, such procedures will not be effective unless combined with implantation of biomaterials to restore the normal shape and pliability of the vibrating edge of the vocal fold and to promote scar-free healing. Early studies suggested the applicability of hydrophilic polymeric materials for reconstruction of vocal cords.[3] Various implantable biomaterials, including Teflon, cross-linked collagen, gelatin, hyaluronic acid, and human abdominal subcutaneous fat, have been used primarily for deep vocal fold augmentation.[4] Most of these materials have drawbacks, such as foreign body reaction, migration, stiffness (Teflon), rapid resorption (collagen, hyaluronic acid and fat), immunological consequences (collagen), and the need for multistage procedures (fat).[5] To date, the leading candidate for a material to serve this function is Hylan B gel (hyaluronic acid cross-linked by divinyl sulfone). Hylan B gel has been the subject of some recent animal studies[6] and clinical experiments[7] with promising results. In addition, benchtop testing has shown that the viscoelasticity of Hylan B gel is a good match to vocal fold tissue.[8] However, a potential drawback is the difficulty of achieving precise injection of a viscous gel through long slender needles into the superficial layers of the vocal fold. We are interested in repairing the damaged vocal folds using a minimally invasive procedure and polymers that can be injected precisely into the injury site and cross-linked in situ.[9] To this end, photo-cross-linkable hydrogels based on the naturally occurring polysaccharide, hyaluronic acid (HA), were investigated.

[†] Massachusetts Institute of Technology.
[‡] H. P. Mosher Laryngological Research Laboratory, Massachusetts Eye and Ear Infirmary.
[§] Brown University.
[⊥] Eaton-Peabody Laboratory, Massachusetts Eye and Ear Infirmary.
[#] Division of Otology & Laryngology, Harvard Medical School.
* To whom correspondence should be addressed: Tel 617-253-3107; Fax 617-258-8827; e-mail rlanger@mit.edu.

10.1021/ma035970w CCC: $27.50
Published on Web 04/02/2004

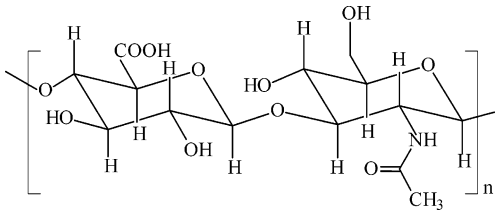

Figure 1. Chemical structure of native hyaluronic acid.

HA (Figure 1) is comprised of β-1,4-linked D-glucuronic acid and β-1,3 *N*-acetyl-D-glucosamine disaccharide units. It is the only nonsulfated glycosaminoglycan (GAG) in the extracellular matrix of all higher animals. It plays pivotal roles in cell differentiation and cell motility. Additionally, HA is inherently angiogenic and plays an active role in wound healing, granulation, and scar remodeling.[10] However, HA, with its β-1,4 backbone linkage and repeated structure of pyranoid rings, has an inherently rigid chain conformation. As a result, hydrogels formed from it may be naturally brittle and cannot retain their structural integrity under high-frequency vibration.[11] For vocal fold applications, it is necessary to be able to fine-tune the rigidity of the polymer backbone in order to match the mechanical properties of the hydrogels to those of the natural tissue. Partial oxidation with periodate offers a method to overcome the chain rigidity; therefore, hydrogels obtained from HA with the open-ring structure may be more elastic.[11]

To further improve HA's applicability for vocal fold regeneration, synthetic polymers can be employed as a building block. The incorporation of synthetic polymers in HA offers a versatile method to fine-tune the properties of the resulting copolymer. The synthetic polymer chosen for this study is poly(2-hydroxyethyl methacrylate) (P(HEMA)). P(HEMA) is a widely studied polymer used in drug delivery, cell encapsulation, dental materials, and contact lenses.[12,13] It is an attractive contender to compensate for the mechanical weaknesses of HA. In addition, the presence of free hydroxyl groups on each repeating unit offers an opportunity for functionalization.

We describe herein photo-cross-linkable hydrogels as potential candidates for vocal fold regeneration. The hydrogels consist of HA directly modified with glycidyl methacrylate (HA/GMA),[14] HA oxidized with periodate followed by conjugation of GMA (HAox/GMA), and HA grafted with oligomeric P(HEMA) before introduction of methacrylate groups (HAox-*g*-P_y)/GMA. Soft and pliable hydrogels were obtained upon UV irradiation in the presence of a photoinitiator. The compositions of the conjugates were confirmed by GPC and ^{1}H NMR. The equilibrium swelling ratio, enzymatic degradation, viscoelastic moduli, and the cross-sectional morphology of the resulting hydrogels were evaluated. Finally, the cell cytotoxicity of both the synthesized macromonomers and the resulting hydrogels was also examined.

Experimental Section

Materials. HA sodium salt (M_w 490 KDa, 1.3 MDa) was provided by Genzyme Corp. (Cambridge, MA). 2-Hydroxyethyl methacrylate (HEMA) and glycidyl methacrylate (GMA) were obtained from Polysciences Inc. (Warrington, PA). Sodium periodate, ethylene glycol, *N*,*N*-dimethylacrylamide (DMAM), 2-aminoethanethiol hydrochloride (AESH), 2,2′-azobis(isobutyronitrile) (AIBN), sodium cyanoborohydride ($NaBH_3CN$), (*N*,*N*-dimethylamino)pyridine (DMAP), tetrabutylammonium bromide (TBAB), 2,2-dimethoxy-2-phenylacetophenone (DMPA), 1-vinyl-2-pyrrolidinone (NVP) and *tert*-butyl carbazate (TBC) were obtained from Aldrich (Milwaukee, WI). Bovine testicular hyaluronidase (HAase, 30 000 U/mg) was obtained from Sigma (St. Louis, MO).

General Methods. ^{1}H NMR spectra were recorded in D_2O at room temperature using a Varian Unity-300 spectrometer. Organic phase gel permeation chromatography (GPC) was performed using a Hewlett-Packard 1100 series isocratic pump, a Rheodyne model 7125 injector with a 100 μL injection loop, and a Phenogel MXL column (5 μm mixed, 300 × 7.5 mm, Phenomenex, Torrance, CA). 70% THF/30% DMSO (v/v) with 0.1 M piperidine was used as the eluent at a flow rate of 1.0 mL/min. Data were collected using an Optilab DSP interferometric refractometer (Wyatt Technology, Santa Barbara, CA) and processed using the TriSEC GPC software package (Viscotek Corp., Houston, TX). The molecular weights and polydispersities of the polymers were determined relative to monodisperse polystyrene standards (Polysciences Inc., Warrington, PA). Aqueous phase GPC was performed using a Pharmacia HPLC pump 2248, a Perkin-Elmer RI detector series 200, a DAWN-EOS MALLS (multiangle laser light scattering detector) (Wyatt Technology, Santa Barbara, CA), and a macrosphere GPC 300 Å column (Alltech, Deerfield, IL). 0.05 M Na_2SO_4 (pH 5) was used as the mobile phase. The system was calibrated with standard HA with known M_w and concentration (Genzyme Corp., Cambridge, MA). Scanning electron microscopy (SEM) was performed on a JSM-6320 FV JEOL SEM. The PBS-swollen hydrogel samples were immersed in water for 1 h and then quickly frozen with liquid nitrogen. The frozen hydrogels were subjected to cryafracturing followed by lyophilization. The dry samples were sputter-coated with palladium and gold (150 Å thick) for SEM examination.

Synthesis of Amino End-Functionalized P(HEMA-*co*-DMAM). Water-soluble P(HEMA) that is end-functionalized with an amino group was prepared by free-radical copolymerization of HEMA and DMAM using AESH as a chain-transferring agent and AIBN as an initiator. Specifically, HEMA (20 mL), DMAM (11 mL), AIBN (0.23 g), and AESH (4.77 g) were dissolved in methanol (200 mL). The solution was bubbled with nitrogen for 30 min at room temperature. The reaction mixture was stirred at 50 °C in a nitrogen atmosphere for 24 h. The polymer was isolated by precipitation into diethyl ether and filtered. The product was further purified by reprecipitation. The solid was dried under vacuum overnight and was examined by GPC and ^{1}H NMR. Yield: 28%.

Preparation of HAox. Hyaluronic acid (M_w 1.3 MDa, 1.0 g, 2.5 mmol) was dissolved in 100 mL of H_2O in a flask that was wrapped with aluminum foil. Sodium periodate (0.6 mmol, 0.2 M in H_2O) was added dropwise, and the reaction was stirred for 2 h at room temperature. Ethylene glycol was then added to inactivate any unreacted periodate. The reaction was stirred for 1 h at ambient temperature. The solution was purified by thorough dialysis (Spectra/Por membrane, MWCO 10 000) against double distilled (dd) water for 3 days. The final dry product was obtained by freeze-drying with a yield of 67%.

Determination of Aldehyde Groups by ^{1}H NMR. The periodate-oxidized HA (HAox) was dissolved in an acetate buffer (pH = 5.2) at a concentration of 10 mg/mL. A 5-fold excess of TBC and $NaBH_3CN$ was dissolved in the same buffer and added separately. The mixture was allowed to react for 24 h at room temperature. The polymer was recovered by precipitation in acetone three times. The polymer was further purified by thorough dialysis against 0.1 M NaCl solution and dd H_2O. The freeze-dried product was subjected to ^{1}H NMR examination, and the aldehyde content was calculated by comparing the signals at 1.4 ppm (9H, carbazate t-Boc) and 1.9 ppm (3H, HAox acetamide).

Synthesis of HAox-*g*-P_y Copolymer. The amine end-functionalized P(HEMA-*co*-DMAM) was coupled to HA by reductive amination using $NaBH_3CN$ as a reducing agent. In a typical experiment, HAox and P(HEMA-*co*-DMAM) (aldehyde/amine molar ratios of 2/1 or 5/1) were dissolved in dd water containing 1 M NaCl to make a 10 mg/mL solution. After

stirring at room temperature for 1 h, $NaBH_3CN$ (4 mol equiv relative to the aldehyde groups) was added. The reaction mixture was stirred for 3 days at room temperature and then precipitated in acetone. The precipitate was dissolved in dd H_2O and subjected to thorough dialysis against dd water (Spectra/Por membrane, MWCO 12 000−14 000). The resulting copolymer was obtained by freeze-drying. The grafting density (y%) was determined by ^{1}H NMR. Yield: 48%.

Synthesis of Photo-Cross-Linkable Conjugates. Photopolymerizable conjugates were prepared by attaching methacrylate groups onto HA, HAox, and HAox-*g*-P_y. Briefly, the polymer was dissolved in water to make a 10 mg/mL solution. 10 mol % (relative to the total hydroxyls in the polymer) DMAP, 20 mol % TBAB, and 10-fold molar excess of GMA were added separately and thoroughly mixed. The reaction was allowed to proceed at room temperature in a nitrogen atmosphere for 24 h. The solution was precipitated in large excess of acetone. The solid that was collected by centrifuge was dissolved in water and thoroughly dialyzed against dd water (Spectra/Por, MWCO of 10 000). A white, fluffy solid was obtained after freeze-drying. The percentage GMA incorporation was determined by ^{1}H NMR.

Hydrogel Formation. To create hydrogels, photo-cross-linkable conjugates were dissolved in PBS at a concentration of 20 mg/mL. The photoinitiator consisted of a 30% solution of DMPA mixed into NVP. 3 μL of photoinitiator solution was added for each 1 mL of macromonomer solution. The solution was exposed to UV irradiation (Black-Ray, UVP Inc., radiation range 315−400 nm, peak at 365 nm) for 10 min.

Equilibrium Swelling Ratio. The as-synthesized hydrogels were dehydrated by passing them through graded ethanol solutions and drying them under vacuum overnight. After the dry weight (W_d) was measured, the dry disks were placed in a PBS buffer for 24 h. The hydrogels were then recovered and blotted with tissue paper before the wet weight (W_s) was measured. The equilibrium swelling ratio (SW) was obtained as the ratio of the wet weight to the dry weight.

Enzymatic Degradation of Hydrogels. Hydrogel disks were incubated in hyaluronidase (HAase) solution (5 U/mL in PBS) at 37 °C with mild mixing on a shaker. The gel mass was monitored daily with the HAase solution refreshed every other day. The time until complete dissolution of the hydrogels was noted.

Mechanical Evaluation. The mechanical properties of the hydrogels were evaluated using an acoustic shaker and laser-Doppler vibrometer in combination with a mathematical model for viscoelastic wave propagation. The hydrogel specimens were placed on the flat upper surface of a Brüel & Kjær (B&K, #4393, Denmark) miniature accelerometer that was mounted on a B&K (#4810) miniature shaker. The accelerometer signal was amplified by a B&K (#2525) measuring amplifier. A 1 mm × 0.5 mm rectangle of reflective tape was placed on the upper surface of the hydrogel. The reflector was firmly attached to the hydrogel by surface tension. A Polytec PI (CA) HLV-100 laser-Doppler vibrometer was used to determine the velocity of the reflector. The reflector localized the reflected light from the upper surface of the translucent hydrogel. The measurements were made using SysId software (SysId Industries, CA) and a DSP16+ (Ariel, NJ) signal-generation and processing board. The stimulus was a chirp containing frequency components of 3−25 000 Hz, repeated every $^1/_3$ s. Simultaneous with the chirp output, two analog-to-digital converters digitized the outputs of the accelerometer's measuring amplifier and the laser-Doppler vibrometer. The averages of 50 stimulus presentations were analyzed by Fourier transforms. The transform of the accelerometer output was converted to velocity using the accelerometer's sensitivity and sinusoidal analysis. The velocity amplification between the top of the specimen, as determined by the laser-Doppler vibrometer, and the base of the specimen, as determined by the accelerometer, was used in the determination of the viscoelastic moduli using the viscoelastic wave analysis described in the Appendix. Additionally, the phase shift between the motion at the top and bottom of the specimen was recorded and used in the comparison with the viscoelastic wave model.

Macromonomer Toxicity and Cell/Hydrogel Interactions. NIH/3T3 cells (ATCC, CRL-1658) were used for toxicity and photoencapsulation studies. Cells were cultured in Dulbecco's Modified Eagle's Medium (Invitrogen) with 4 mM L-glutamine adjusted to contain 1.5 g/L sodium bicarbonate and 4.5 g/L glucose and supplemented with 10% calf serum and 1% antibiotics (Invitrogen). Cells were trypsinized and seeded into 24-well plates at a density of 10 000 cells/well in 1 mL of culture media. After seeding, 100 μL of a solution containing the synthesized macromonomers, unmodified hyaluronic acid, or no macromonomer in phosphate buffered saline (PBS) was added to each well to bring the final monomer concentration in the culture media to 0.002, 0.02, 0.2, or 2.0 mg/mL. The relative toxicity of the monomers on the NIH/3T3 cells was assessed with a commercially available MTT viability assay (ATCC, 30-1010K) after 3 days of culture without changing the media. For this assay, 100 μL of the MTT reagent (tetrazolium salt solution) was added directly to the wells, and the plate was placed in an incubator at 37 °C for 4 h. The purple formazen produced by active mitochondria was solubilized with the addition of 1 mL of the provided detergent solution followed by orbital shaking for 2 h. The absorbance of these solutions was then read at 570 nm (Molecular Devices SpectraMax 384). Results are reported as the average ($n = 3$) and standard deviation of the measured absorbance normalized to the absorbance of NIH/3T3 cells cultured in unmodified media.

To assess the viability of photoencapsulated cells, NIH/3T3 cells were suspended (50 million cells/mL) in a solution of the HA-*g*-P(HEMA-*co*-DMAM) macromonomer (20 mg/mL) and 0.05 wt % Darocure 2959 (2-hydroxy-1-[4-(hydroxyethoxy)-phenyl]-2-methyl-1-propanone) in PBS. 50 μL of the suspension was introduced into a sterile mold and polymerized with exposure to ∼6 mW/cm^2 ultraviolet light (Blak-Ray, model B100AP) for 10 min. The polymerized cell/gel constructs were placed in culture media, and the toxicity of the photoencapsulated cells was assessed using the MTT assay immediately after encapsulation (day 0) and after 3 and 7 days of culture. The media was changed on the gels every other day. Prior to measuring the absorbance, cell/gel constructs were homogenized using disposable tissue homogenizers (VWR). Results are reported as the average ($n = 3$) and standard deviation of the measured absorbance.

Results and Discussion

Macromonomer Synthesis. Chemical modification of HA has been studied for a variety of applications. HA contains both carboxylic acid and hydroxyl groups that are readily modified with reactive groups.[15] Periodate treatment oxidizes the proximal hydroxyl groups to aldehyde, which opens the sugar ring to form a linear chain, thus giving rise to a more flexible polymer backbone. The aldehyde groups can be used as reactive handles for attachment of synthetic polymers and/or cell adhesive peptides. The degree of oxidation can be controlled easily by the relative amount of periodate added.[16] To quantify the aldehyde content, the oxidized HA was allowed to react with excess *tert*-butyl carbazate under acidic conditions at room temperature for 24 h. The unreacted carbazate was removed by repetitive precipitation and subsequent dialysis. The ^{1}H NMR spectrum of the product shows two well-resolved singlet peaks at 1.4 and 1.9 ppm that are attributed to carbazate *t*-Boc and HAox acetamide, respectively. When an equal molar amount of $NaIO_4$ was used, the viscosity of the reaction solution decreased dramatically after the 2 h reaction, indicating a high degree of oxidation and partial degradation. When HA of M_w 1.3 MDa was used, a M_w of 260 kDa was observed by aqueous GPC for the oxidized product with 70% dialdehyde groups per disaccharide unit. On the other hand, when 25 mol % $NaIO_4$ was used, the reaction solution remained viscous

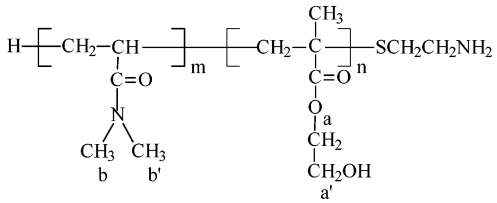

Figure 2. Chemical structure of semitelechelic P(HEMA-*co*-DMAM) with amino group.

Table 1. Synthetic Results of P(HEMA-*co*-DMAM) with Amino End Group[a]

	$[M_1]/[M_2]$			M_n	M_w	
[S]/[M]	in feed	in product	[I]/[M]	(g/mol)	(g/mol)	PDI
0.15	60:40	69:31	0.005	7307	10397	1.4

[a] M_1 = HEMA; M_2 = DMAM; [M] = $[M_1]$ + $[M_2]$; I = AIBN; S = AESH; PDI = M_w/M_n.

and the M_w of the partially oxidized HA was 650 kDa with a dialdehyde concentration of 16%. A relatively low degree of modification was desired to retain the beneficial properties of native HA. Therefore, 16% oxidation was chosen for the subsequent studies.

To obtain hydrogels with a wide range of properties, HA was grafted with a synthetic polymer of P(HEMA). To this end, a semitelechelic copolymer of HEMA and DMAM was synthesized. Semitelechelic polymers containing a reactive group at one end of the polymer chain have been used for conjugation or grafting reaction to other species or surfaces.[17,18] In this study, 2-aminoethanethiol (AESH) was used as a chain transfer agent to prepare a semitelechelic polymer with an amino end group (Figure 2). DMAM was used as a comonomer to enable both water solubility and dilution of hydroxyl groups on P(HEMA). The resulting polymer has a random distribution of the comonomers and is readily soluble in H_2O, methanol, DMF, and a mixture of THF/DMSO (7/3, v/v). The polymerization results are summarized in Table 1. It is clear that oligmeric P(HEMA-*co*-DMAM) was obtained in the presence of AESH and that the polydispersity falls within the range of a typical radical polymerization. The ^{1}H NMR spectrum of the copolymer shown in Figure 3B verifies the chemical composition of the copolymer. The peaks at 3.1−2.6 ppm (6H) represent the methyl protons of the amide function of DMAM (H^b and $H^{b'}$ as shown in Figure 2). The signals at 3.7 and 4.0 ppm (4H) are attributed to the ester methylene protons of the HEMA unit (H^a and $H^{a'}$ as shown in Figure 2), and the percentage of HEMA in the copolymer was calculated to be 69 mol % based on the integration areas of the corresponding peaks. Previous work has shown that under the same experimental condition one oligo-HEMA molecule has approximately one amino group at one end of the chain.[19] Our ^{1}H NMR spectrum of the copolymer obtained in DMSO-d_6 (not shown) clearly indicates the presence of the amino groups.

P(HEMA-*co*-DMAM) was then grafted to HAox through reductive amination using $NaBH_3CN$ as the reducing agent. The resulting copolymer is referred to as HAox-*g*-P_y, where *y*% indicates the percentage grafting of P(HEMA-*co*-DMAM). The reaction condition was chosen to minimize the degradation of HAox and to introduce a relatively small amount of P(HEMA-*co*-DMAM) to preserve the native characteristics of HA. After thorough purification and freeze-drying, the copolymer was obtained as a white, fluffy solid. It is worth

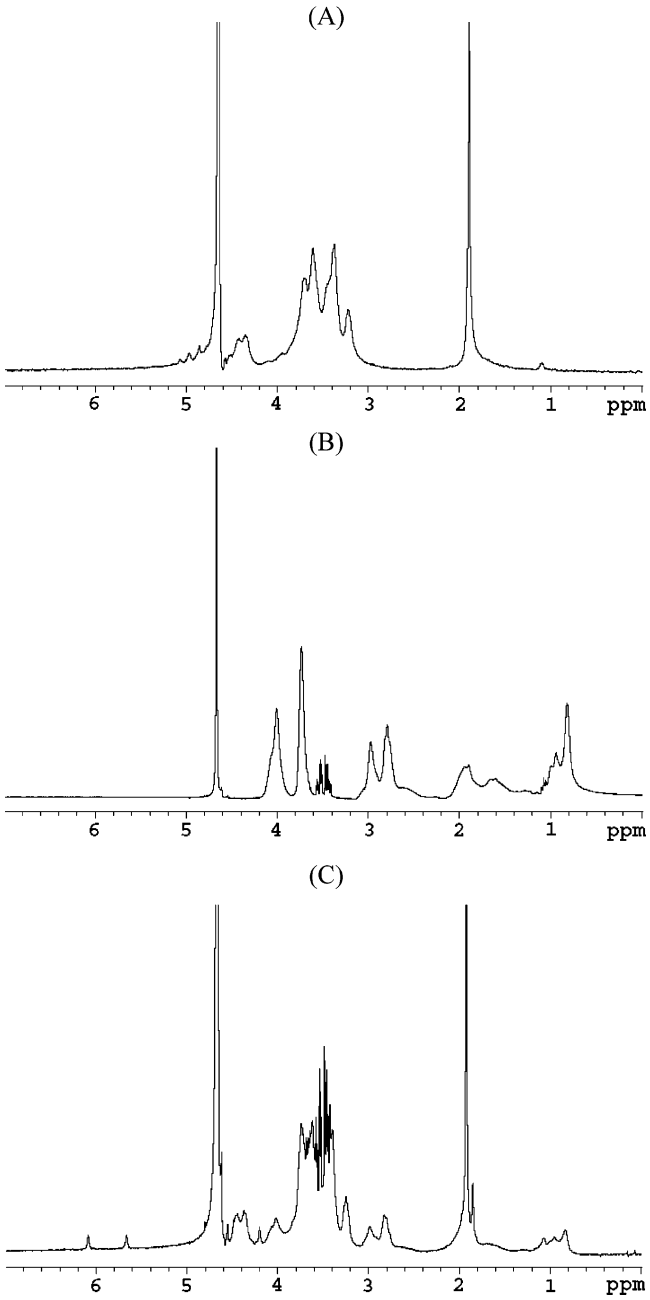

Figure 3. ^{1}H NMR spectra of HAox (A), P(HEMA-*co*-DMAM) (B), and (HAox-*g*-$P_{1.9}$)/GMA (C) in D_2O.

mentioning that the copolymer with 1.9% P(HEMA-*co*-DMAM) grafting density is soluble in water and a water/methanol (1:1) mixture. As indicated before, P(HEMA-*co*-DMAM) is soluble in both water and methanol, while HA and HAox are only soluble in water. The solubility change after the reaction indicated successful grafting of the P(HEMA-*co*-DMAM) to HA. The ^{1}H NMR spectrum of the graft copolymer also confirms the covalent attachment of P(HEMA-*co*-DMAM).

Photo-cross-linkable conjugates were prepared by reacting HA, HAox, or HAox-*g*-P_y with a 10-fold excess (relative to the available hydroxyls) of glycidyl methacrylate (GMA) in aqueous solution in the presence of tertiary amine and a phase transferring agent. GMA reacts with hydroxyl groups both on HA and HEMA (Figure 4). ^{1}H NMR spectra for HA/GMA and HAox/GMA presented the typical characteristic signals of HA

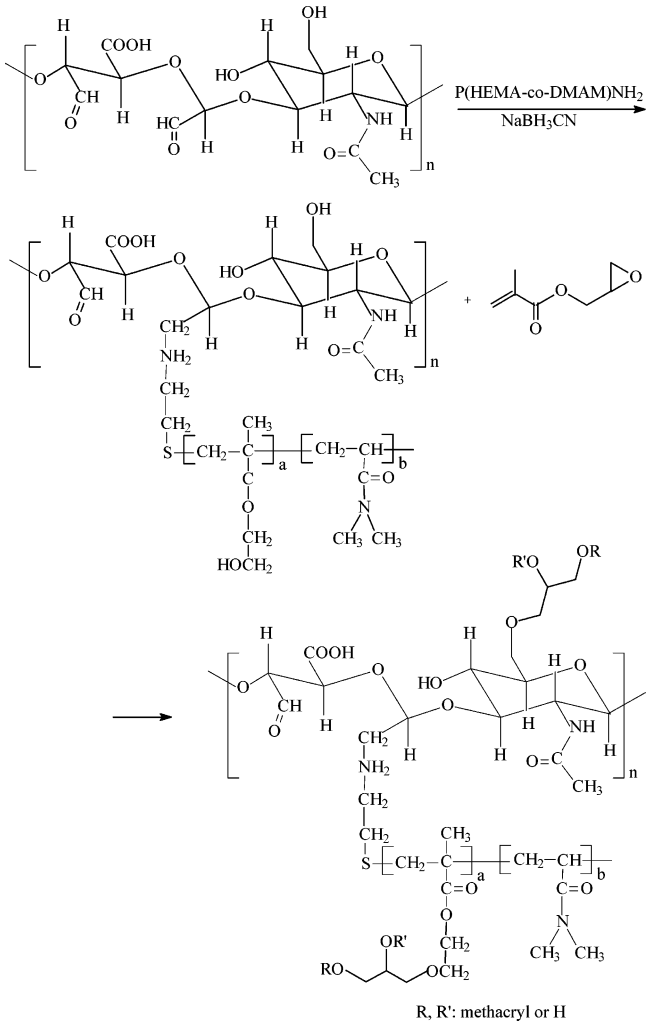

Figure 4. Synthesis of (HAox-*g*-P_y)/GMA conjugate.

and GMA: HA, δ 1.9 ppm (NAc−CH_3), 3.3−3.9 ppm (H-2,3,4,5,6), 4.4−4.6 (H-1); GMA: δ 5.6 and ∼6.1 ppm (CH_2═C), 1.8 ppm (C−CH_3). The approximate percentage of methacrylation can be calculated from the relative integrations of the methacrylate protons and HA's methyl protons. ^{1}H NMR spectrum for (HA-*g*-$P_{1.9}$)/GMA showed additional signals from P(HEMA-*co*-DMAM) as well as those described above (Figure 3C): δ 1.2−0.8 (backbone CH_2 from DMAM and backbone CH_3 from HEMA), 3.1−2.6 (C(O)N(CH_3)$_2$ of DMAM), and δ around 4 ppm (C(O)CH_2CH_2OH in HEMA). From the signal ratio of amide methyl protons (3.1−2.6 ppm) of oligmeric copolymer to the protons at H-1 of HAox (4.4−4.6 ppm), the grafting percent of P(HEMA-*co*-DMAM) in the copolymer was determined. Since GMA can react with the hydroxyls of HA as well as those of the HEMA repeating unit in the graft, it is difficult to estimate the relative amount of GMA incorporation in each of the components. Therefore, the amount of methacrylate groups in the conjugate was normalized to HA.

Table 2 summarizes the characterization of the photo-cross-linkable conjugates and the resulting hydrogels. The percentage P(HEMA-*co*-DMAM) grafting varies from 0 to ∼2%, while the amount of methacrylate groups incorporated varies from 8 to 25%. A decrease in molecular weight was seen for reactions involving HAox, and it was attributed to the susceptibility of the oxidized HA to hydrolytic degradation.[20] There was also a slight molecular weight drop when virgin HA (M_w of 490 kDa) was treated with GMA, which has been reported before.[14]

Table 2. Characterization of Photo-Cross-Linkable Polymer Conjugates and the Resulting Hydrogels

	macromonomer				hydrogel		
sample[a]	M_w (kDa)	M_n (kDa)	graft (%)[b]	GMA (%)[c]	f_1 (Hz)[d]	E_1 (Pa)[e]	(tan δ)$_1$[f]
A	320	260	0	8	49	1210	0.075
B	415	305	0	11	85−104	3240	0.075
C	220	160	0.5	13	76−95	2780	0.102
D	245	185	1.9	25	94	5540	0.069

[a] A = HAox/GMA, B = HA/GMA, C = (HAox-*g*-$P_{0.5}$)/GMA, and D = (HAox-*g*-$P_{1.9}$)/GMA. [b] P(HEMA-*co*-DMAM) grafting percent. [c] Percentage GMA incorporation relative to HA. [d] First resonance frequency measured by the acoustic shaker. [e] Elastic modulus at frequency f_1. [f] tan δ at frequency f_1.

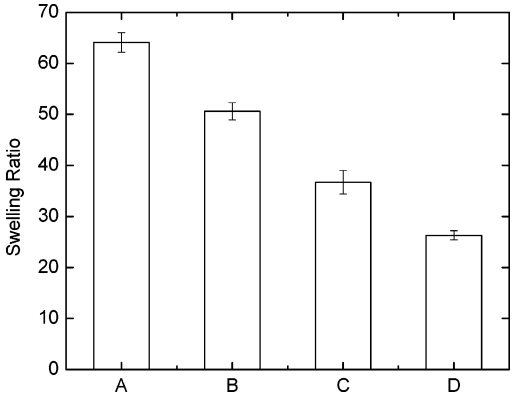

Figure 5. Equilibrium swelling ratio for HA based hydrogels: HAox/GMA (A), HA/GMA (B), (HAox-*g*-$P_{0.5}$)/GMA (C), and (HAox-*g*-$P_{1.9}$)/GMA (D).

Equilibrium Swelling and Enzymatic Degradation of Hydrogels. Soft and flexible hydrogels were obtained after exposing the aqueous polymer solution to UV irradiation for 10 min in the presence of a photoinitiator. To assess the swelling properties of these hydrogels, the equilibrium swelling ratio, SW, was determined. Swelling influences solute diffusion, surface properties, and mechanical stability of a hydrogel. Thus, the swelling ratio is an important parameter to evaluate the cross-linking density of the hydrogel networks. Since the hydrogel matrices are composed of charged HA, it is obvious that the SW values will change depending on the type of solution used. All measurements were made by immersing hydrogels in PBS of pH 7.4. All hydrogels reached equilibrium swelling in 3 h. As shown in Figure 5, HAox with 8% methacrylation exhibits the highest swelling ratio, indicating that it has the least dense network. HA with 11% methacrylation gives a SW of 50, whereas HAox grafted with 0.5% P(HEMA-*co*-DMAM) and 13% GMA swells to a lesser extent. HAox grafted with 1.9% P(HEMA-*co*-DMAM) and 25% GMA yields the smallest SW. The difference in swelling ratio was attributed to the variation in GMA content and the presence of grafted P(HEMA-*co*-DMAM) chains. In this system, a 1.9% grafting density is calculated to correspond to 0.89 HEMA repeating unit for every disaccharide unit. It is, therefore, highly possible that the steric bulk of the grafted P(HEMA-*co*-DMAM) chains acts as a protective shield against water and other reagents. Although HEMA is water-soluble, P(HEMA) is not. Therefore, the grafted chains are less hydrophilic than the HA back-

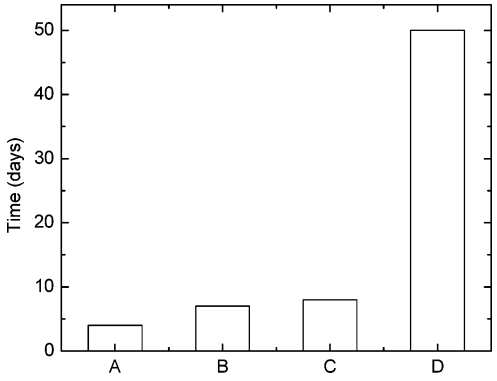

Figure 6. In vitro enzymatic degradation of HA-based hydrogels: HAox/GMA (A), HA/GMA (B), (HAox-*g*-$P_{0.5}$)/GMA (C), and (HAox-*g*-$P_{1.9}$)/GMA (D).

bone, which makes the conjugate more hydrophobic. Finally, the incorporation of P(HEMA) onto the HA backbone amplifies the total amount of active hydroxyl groups that can further react with GMA, leading to a tighter network.

Hyaluronic acid is naturally degradable by hyaluronidase (HAase) and inflammation-generated active oxygen in the form of hydroxyl radicals.[21,22] The goal of this study is to synthesize in situ cross-linkable hydrogels with prolonged residence time, yet biodegradable in the long-term to allow for replacement by the regenerated tissue. In vitro degradation was studied by incubating hydrogels in a 5 U/mL HAase/PBS solution and monitoring the gel mass over time. The enzyme concentration was chosen to approximate endogenous levels.[14] Initially, the cylindrically molded hydrogels exhibited defined sharp edges. These edges changed to smooth, rounded edges after incubation in HAase/PBS at 37 °C for extended periods of time, indicating enzymatic degradation. The gel mass (wet weight) increased during the early stage of degradation which can be attributed to the increase in swelling due to the loss of unreacted macromonomer. Later, the network disintegrated to such an extent that it could no longer hold a large amount of water and the gel mass decreased. Eventually, the hydrogels disintegrated and an aqueous solution was left. The time required for the complete disappearance of hydrogel disks was used to assess their degradability. Figure 6 shows degradation properties of the hydrogels synthesized in this study. It is clear that HAox/GMA degraded most readily, while HAox grafted with 1.9% P(HEMA-*co*-DMAM) and 25% GMA did not completely dissolve in 50 days. It is worth emphasizing that the presence of 0.5% P(HEMA-*co*-DMAM) did not substantially alter the degradation rate of the hydrogel, whereas 1.9% P(HEMA-*co*-DMAM) grafting dramatically increased its resistance to enzymatic degradation. These results suggest that the accessibility of HAase to the HA chain may be inhibited by its entanglement with the grafted P(HEMA-*co*-DMAM) chains. Further, the presence of a photo-cross-linkable moiety in both the HAox backbone and the HEMA side chain repeating units probably resulted in a tighter network, further reducing the accessibility of HAase. All hydrogel samples were clearly present after 2 months in an enzyme-free PBS buffer, although an increase in the gel mass was observed during this period. The rapid degradation of HAox/GMA by HAase demonstrates that HAase can recognize and process HA backbones partially oxidized by $NaIO_4$.

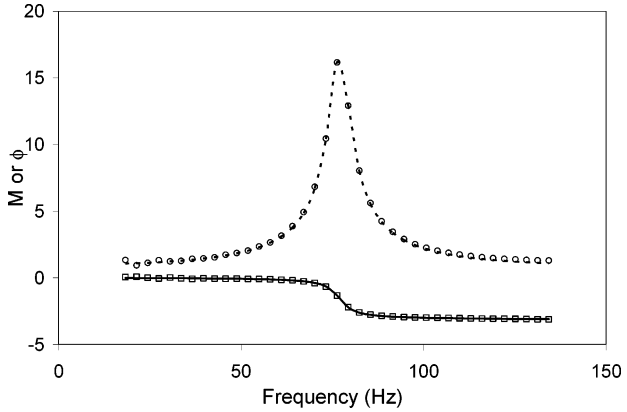

Figure 7. Comparison between theoretical prediction and experimental data for amplification factor (M) and phase shift (ϕ) as a function of frequency: (···) M from theory; (○) M from experiment; (—) ϕ from theory; (□) ϕ from experiment.

Mechanical Characterization of Hydrogels. The mechanical properties of the photo-cross-linked hydrogels were evaluated using a novel vibrational method to assess their applicability for vocal fold regeneration. A cylindrical hydrogel specimen was subjected to small-amplitude longitudinal vibration using an acoustic shaker. The amplification factor (the amplitude of the velocity at the top of the hydrogel relative to the velocity of the shaker surface) was measured as a function of frequency using a laser-Doppler vibrometer as described previously. Published data on the viscoelastic properties of hydrogels are typically limited to frequencies of up to 15 Hz.[23,24] The instrumentation used here can make accurate velocity measurements over a wide frequency range (15−1000 Hz in our application).[25,26] The frequency at which the amplification factor reaches a local maxima corresponds to a resonance frequency of the hydrogel sample. Using a longitudinal vibration model (see Appendix) for a slender viscoelastic rod of known length and density, the complex viscoelastic moduli of the hydrogels were derived by matching the first observed resonance peak (at frequency f_1) with the parameters of the viscoelastic model. The results indicate that the agreement in the amplification factor and the phase shift is excellent over the range of frequencies near f_1 (Figure 7). Figure 8 shows the real part (E_1) of the complex modulus and the viscosity (η) of the hydrogels near f_1. For all hydrogel samples studied, E_1 increased slightly with increasing frequency while η decreased with increasing frequency. Such behavior is consistent with common findings for soft biological tissues and polymeric materials.[27] HAox/GMA hydrogels exhibited the lowest elastic stiffness and viscosity. (HAox-*g*-$P_{1.9}$)/GMA hydrogels showed the highest stiffness followed by HA/GMA and (HAox-*g*-$P_{0.5}$)/GMA. On the other hand, HA/GMA hydrogels gave a higher viscosity than (HAox-*g*-$P_{0.5}$)/GMA hydrogels. It is known that the viscoelastic properties of polymeric materials depend on the ease of molecular movement, which is determined by the number and strength of molecular interactions such as physical entanglement, electrostatic forces, hydrophobic/hydrophilic interactions, and chemical cross-linking.[27,28] The relative stiffness of the polymeric chains also plays an important role.[11] HAox/GMA hydrogels are expected to have the lowest cross-linking density due to their relatively low GMA content. In addition, periodate oxidation of HA should give rise to a more flexible polymer backbone due to the reduced steric

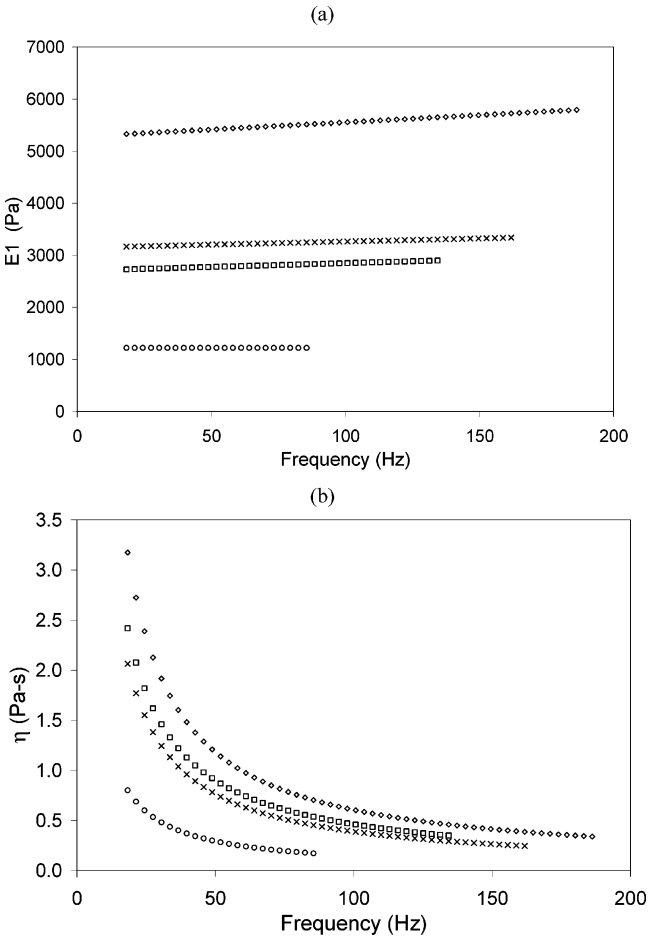

Figure 8. Real part of the complex viscoelastic modulus (E_1, a) and viscosity (η, b) as a function of frequency for HA-based hydrogels: HAox/GMA (○), HA/GMA (×), (HAox-*g*-$P_{0.5}$)/GMA (□), and (HAox-*g*-$P_{1.9}$)/GMA (◇).

hindrance to the rotation of glycosidic linkage. Our observation that HAox/GMA hydrogels are the softest is consistent with this interpretation. We also found that (HAox-*g*-$P_{0.5}$)/GMA and (HAox-*g*-$P_{1.9}$)/GMA are stiffer than HAox/GMA hydrogels, with (HAox-*g*-$P_{1.9}$)/GMA being the stiffest. This might be explained by an increase in physical entanglement, which is further locked in by chemical cross-linking. The grafted chains could restrict the free rotation of the HAox backbone, thereby reducing the chain flexibility. The higher GMA incorporation for (HAox-*g*-$P_{0.5}$)/GMA and (HAox-*g*-$P_{1.9}$)/GMA should also lead to tighter networks. Compared with HAox/GMA, HA/GMA has higher molecular weight as well as higher GMA content but lacks the open-ring structure. Therefore, it is understandable that HA/GMA hydrogel showed higher E_1 values.

The viscoelasticity of human vocal fold lamina propria has been studied using parallel plate rheometers with small-amplitude shear oscillation at frequencies ranging from 0.01 to 15 Hz.[29] A direct comparison of the hydrogels investigated in this paper with the natural tissue, however, is not possible due to the difference in the frequency range and the mode of deformation. Since the frequency range of human phonation is above 100 Hz, the high-frequency viscoelastic response is of great interest. The mechanical evaluations of vocal fold tissue before and after hydrogel injection are currently being explored using a torsional wave approach that is expected to measure the response of both vocal fold tissue and scaffold materials at high frequencies.

SEM Characterization of Hydrogels. The morphologies of the fully swollen hydrogels were examined by SEM. The introduction of covalent cross-linking was expected to produce three-dimensional networks. The high water content of the hydrogels suggests that upon lyophilization highly macroporous spongelike scaffolds should be produced. Figure 9 shows the SEM images of freeze-dried hydrogel samples. HAox/GMA hydrogel exhibited a predominantly fibrous structure with occasional sheetlike entities. Close inspection of the image of HA/GMA hydrogel samples suggested a collapsed morphology probably due to the mechanical stress generated during sample preparation and measurement. The presence of a continuous porous structure is clearly observable, which may have been distorted by the collapsing of the matrix. HAox-*g*-P_y/GMA samples had continuous circular or hexagonal pores, with an average diameter of 30 μm. The morphologies observed by SEM may offer insights into the physical properties of the hydrogels. A relatively large surface area is associated with fiber-rich structures. Therefore, the HAox/GMA network can hold more water and is widely open for enzymes to attack, thus showing a higher swelling ratio and faster degradation. However, no correlation between the degradation profiles and the network morphologies was apparent for other hydrogel samples. The porous structures observed for these hydrogels suggest their potential as scaffolds for cell infiltration and growth.

Cell Cytotoxicity. As a further measure of the applicability of the synthesized hyaluronic acid-based hydrogels for vocal fold regeneration, the cell cytotoxicity was assessed for both un-cross-linked macromonomer solutions and photo-cross-linked hydrogels. A fibroblast cell line, NIH/3T3, was used for these initial cytotoxicity studies. The results were normalized to the absorbance of cells cultured in normal media. Unmodified HA (M_w 490 kDa) was used as the control since it is well-known to be biocompatible.[10] As shown in Figure 10, no significant difference in cell viability (assessed by an MTT mitochondrial activity assay) was seen between HAox/GMA and HA solutions at low concentration (0.002−0.2 mg/mL) after 3 days of culture. This observation indicates that partial oxidation and GMA conjugation did not have an adverse effect on cells. A previous study indicated that HA/GMA was cytocompatible.[14] A decrease in cell viability was measured for (HAox-*g*-$P_{1.9}$)/GMA solutions. The observed absorbance decreased as the macromonoer concentration increased. It is possible that there were trace amounts of low molecular weight reagents that were not completely removed by the purification process employed here for (HAox-*g*-$P_{1.9}$)/GMA. Further purification may be necessary for future applications as biomaterials. For all three samples tested, a significant decrease in cell viability was seen at the highest monomer concentration (2 mg/mL). It should be emphasized that there is considerable difference between the in vivo and in vitro environments. Exposing the cells to these concentrations in a stagnant environment for several days should be the worst case scenario.

To assess the viability of cells photoencapsulated in the HA-based networks, the NIH/3T3 cells were encapsulated in the (HAox-*g*-$P_{1.9}$)/GMA macromonomer with exposure to mild ultraviolet light in the presence of a water-soluble photoinitiator. These initiating systems were previously determined to be cytocompatible.[30] This

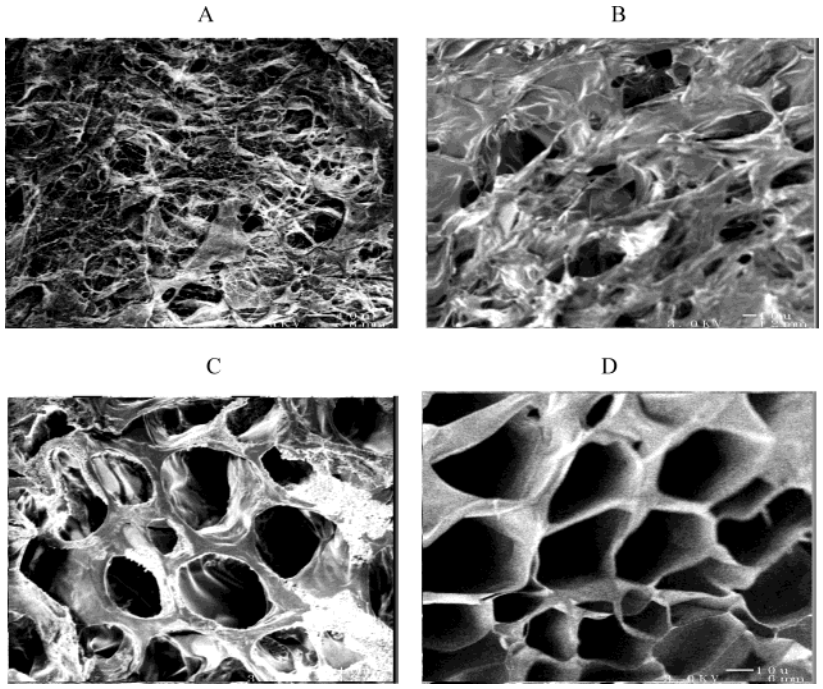

Figure 9. SEM micrographs of HA-based hydrogels: HAox/GMA (A), HA/GMA (B), (HAox-*g*-$P_{0.5}$)/GMA (C), and (HAox-*g*-$P_{1.9}$)/GMA (D).

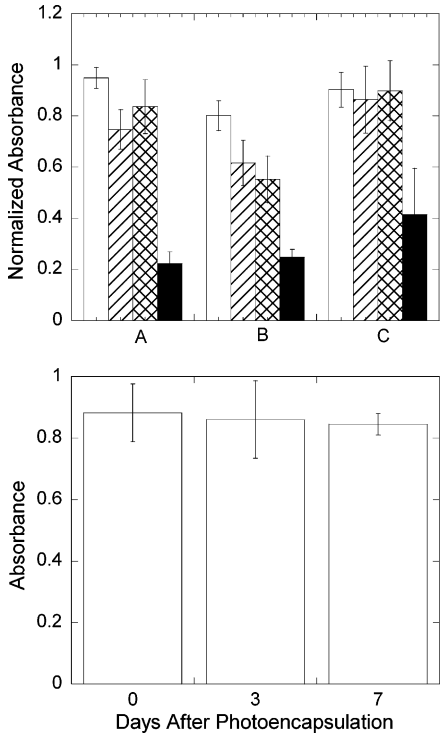

Figure 10. (top) Viability of NIH/3T3 cells cultured for 3 days in the presence of HAox/GMA (A), (HAox-*g*-$P_{1.9}$)/GMA (B), or unmodified HA (C) at concentrations of 0.002 (white), 0.02 (striped), 0.2 (diamond), and 2.0 mg/mL (black). (bottom) Viability of NIH/3T3 cells photoencapsulated in (HAox-*g*-$P_{1.9}$)/GMA immediately after encapsulation and after 3 and 7 days of in vitro culture as measured by an MTT viability assay.

macromonomer was chosen because it correlates with the largest decrease in cell viability in the previous study. As shown in Figure 10, there was no significant change in the overall cell viability immediately after encapsulation and after 3 and 7 days of culture. These results imply that there is little toxicity in the reacted hydrogel networks. It is possible that the presence of a 3-dimensional network reduced the direct exposure of cells to the low molecular weight toxic reagents. It may also be possible that the trace amount of toxic reagent within the gel was leached out during the experiments.

Conclusion

This work has investigated the photo-cross-linking characteristics and material properties of a series of hyaluronic acid-based materials for potential use in vocal fold augmentation. The matrix polymers studied include native HA, partially oxidized HA (HAox), and P(HEMA-*co*-DMAM) grafted HA (HAox-*g*-P_y/GMA). A low degree of HA modification was emphasized in order to retain its intrinsic characteristics. Subsequent reaction with glycidyl methacrylate (GMA) resulted in photo-cross-linkable conjugates that can be converted into soft and flexible hydrogels upon UV irradiation in the presence of a photoinitiator. HAox/GMA hydrogels exhibited the highest swelling ratio and degraded most readily. Hydrogels obtained from (HAox-*g*-$P_{1.9}$)/GMA were most resistant to enzymatic degradation. Mechanical tests under voicelike vibration conditions yielded the complex viscoelastic moduli of the hydrogels. Among the hydrogels studied, (HAox-*g*-$P_{1.9}$)/GMA was the stiffest and HAox/GMA was the softest. SEM cross-sectional images revealed the fibrous or porous morphology of the fully swollen hydrogels. Finally, the viability of photoencapsulated NIH/3T3 cells did not change with culture time. In vivo evaluation regarding the applicability of these hydrogels for vocal fold augmentation is in progress.

Acknowledgment. This work was generously supported by the Eugene B. Casey Foundation and the Advisory Board Foundation. The authors thank Genzyme Corp. for providing hyaluronic acid and Dr. Laura Yang of Genzyme Corp. for aqueous GPC measurements.

Appendix

Determination of Complex Modulus from Longitudinal Vibration Experiments. Consider the lon-

gitudinal vibration of a slender viscoelastic rod of length h. Let the bottom of the rod be subjected to a sinusoidal oscillation such that the velocity at its base $x = 0$ is given by

$$u(0,t) = u_0 \exp(i\Omega t) \tag{A.1}$$

where u_0 is a constant amplitude and Ω is a constant frequency. The motion of the rod is governed by the dynamical equation of motion

$$\sigma_x = \rho u_t \tag{A.2}$$

where ρ is the mass density and $\sigma = \sigma(x,t)$ and $u = u(x,t)$ are respectively the normal stress and longitudinal velocity at position x at time t. Partial derivatives with respect to position x and time t are indicated by the respective subscripts. The velocity u satisfies the compatibility requirement

$$u_x = \epsilon_t \tag{A.3}$$

where $\epsilon = \epsilon(x,t)$ is the longitudinal strain. For a linear viscoelastic rod the constitutive equation relating the stress and strain histories can be written in the form[27]

$$\sigma(x,t) = \int_0^t E(t - t')\, \epsilon_t(x,t')\, \mathrm{d}t' \tag{A.4}$$

where $E(t)$ is the relaxation modulus for the viscoelastic material and $\epsilon(x,t)$ is assumed to vanish for all times before $t = 0$. Because the end of the rod $x = h$ is a free end, the stress must satisfy the boundary condition

$$\sigma(h,t) = 0 \tag{A.5}$$

The system of eqs A1−A5 can be solved by the method of Laplace transformation[31] to obtain the velocity of the free end in the form

$$u(h,t) = M(\Omega) u_0 \cos(\Omega t - \phi(\Omega)) \tag{A.6}$$

in which $M(\Omega)$ is the amplification factor

$$M(\Omega) = \frac{1}{\sqrt{\cos^2[\xi(\Omega)\, \alpha(\Omega)] + \sinh^2[\xi(\Omega)\, \beta(\Omega)]}} \tag{A.7}$$

and $\phi(\Omega)$ is the phase shift defined by

$$\tan(\phi(\Omega)) = \tan(\xi(\Omega)\, \alpha(\Omega)) \tanh(\xi(\Omega)\, \beta(\Omega)) \tag{A.8}$$

where

$$\xi(\Omega) = \Omega h \sqrt{\frac{\rho}{|E^*(\Omega)|}}$$

$$\alpha(\Omega) = \cos\left[\frac{\delta(\Omega)}{2}\right]$$

$$\beta(\Omega) = \sin\left[\frac{\delta(\Omega)}{2}\right]$$

in which $|E^*(\Omega)|$ and $\delta(\Omega)$ are respectively the magnitude and the phase angle of the complex modulus:

$$E^*(\Omega) = |E^*(\Omega)| e^{i\delta(\Omega)} \tag{A.9}$$

The complex modulus is related to the Laplace transform[31]

$$\tilde{E}(s) = \int_0^\infty \exp(-st) E(t)\, \mathrm{d}t \tag{A.10}$$

of the relaxation modulus $E(t)$ through[32]

$$E^*(\Omega) \equiv i\Omega \tilde{E}(i\Omega) \tag{A.11}$$

The amplification factor is smallest near the zeroes of $\cos(\xi(\Omega)\, \alpha(\Omega))$, i.e., at frequencies Ω_n that satisfy

$$\xi(\Omega_n)\, \alpha(\Omega_n) = \frac{n\pi}{2}, \quad n = \pm 1, \pm 3, \ldots \tag{A.12}$$

As the driving frequency is increased, large amplitude motion at $x = h$ occurs first at $\Omega = \Omega_1$. Measurement of the amplification and phase shift at frequencies near those for which these large motions occur provides information on the complex modulus of the material. Thus, we use eq A7−A9 to determine $|E^*(\Omega)|$ and $\delta(\Omega)$ over a range of frequencies near Ω_1 by finding the values of the complex moduli that provide the best agreement between predicted and measured values of $M(\Omega)$ and $\phi(\Omega)$ over the corresponding range of frequencies. Two approaches have been used. In one approach the relaxation modulus $E(t)$ was represented by a collocation model:[32,33]

$$E(t) = C_\infty + \sum_{i=1}^{n} C_i \exp(-t/t_i) \tag{A.13}$$

where $C_\infty \equiv E(\infty)$ is the late time or "rubbery" modulus for the viscoelastic material, and C_i, t_i are parameters to be evaluated to provide a best fit to the experimental results. Although the number of terms n was taken to be three, very good agreement was found over the amplification peak associated with the first mode by using only the three parameters associated with $n = 1$. We also used a regression-analysis approach in which $|E^*(\Omega)|$ and $\delta(\Omega)$ were taken to vary linearly from their values at Ω_1. Because $\delta(\Omega)$ is normally reported to vary slowly with frequency,[27] we reduced the number of parameters from four to three by taking $\delta(\Omega)$ to be constant. Again, very good agreement was obtained with the experimental records over the amplification peak associated with the first mode for all samples. While the values of $|E^*(\Omega_1)|$ and $\delta(\Omega_1)$ were essentially the same for the two approaches, there were significant differences in the variation of $|E^*(\Omega)|$ and $\delta(\Omega)$ with frequency at frequencies near Ω_1. We adopted the regression analysis approach because taking $\delta(\Omega)$ to be constant appears to be most consistent with results reported for other polymers.[27] In presenting the results we replace the circular frequency Ω by the frequency $f = \Omega/(2\pi)$.

Viscoelastic moduli for the four compositions described herein are shown in Figure 8, where the real part, $E_1(f)$, and the viscosity, $\eta(f)$, of the complex moduli, i.e.

$$E^*(f) = E_1(f) + i2\pi f\, \eta(f) \tag{A.14}$$

are shown in parts a and b, respectively. Because the parameter values are determined primarily by the experimental response near the respective first peaks in the measured amplification factors, viscoelastic properties shown in Figure 8 should be viewed as primarily indicative of material response at these peaks—which

occur at approximately the mid frequency of the frequency ranges shown for each material in Figure 8.

References and Notes

(1) Zeitels, S. M.; Hillman, R. E.; Desloge, R. B.; Mauri, M.; Doyle, P. B. *Ann. Otol. Rhinol. Laryngol. Suppl.* **2002**, *190*, 21.
(2) Zeitels, S. M. *Atlas of Phonomicrosurgery and Other Endolaryngeal Procedures for Benign and Malignant Disease*; Singular: San Diego, 2001.
(3) Peppas, N. A.; Benner, R. E., Jr. *Biomaterials* **1980**, *1*, 158.
(4) Chan, R. W.; Titze, I. R. *Laryngoscope* **1999**, *109*, 1142.
(5) Hallén, L.; Testad, P.; Sederholm, E.; Dahlqvist, Å.; Laurent, C. *Laryngoscope* **2001**, *111*, 1063.
(6) Hallen, L.; Johansson, C.; Laurent, C. *Acta Otolaryngol.* **1999**, *119*, 107.
(7) Hertegard, S.; Hallen, L.; Laurent, C.; Lindstrom, E.; Olofsson, K.; Testad, P.; Dahlqvist, A. *Laryngoscope* **2002**, *112*, 2211.
(8) Hertegard, S.; Dahlqvist, A.; Laurent, C.; Borzacchiello, A.; Ambrosio, L. *Otolaryngol Head Neck Surg.* **2003** *128*, 401.
(9) Anseth, K. S.; Burdick, J. A. *Mater. Res. Soc. Bull.* **2002**, *27*, 130.
(10) Laurent, T. C., Ed. *The Chemistry, Biology, and Medical Applications of Hyaluronan and Its Derivatives*; Portland Press: London, 1998.
(11) Lee, K. Y.; Bouhadir, K. H.; Mooney, D. J. *Biomacromolecules* **2002**, *3*, 1129.
(12) Peppas, N. A.; Moyniham, H. J. In Peppas, N. A., Ed. *Hydrogels in Medicine and Pharmacy*; CRC Press: Boca Raton, FL, 1987; Vol. 2.
(13) Pedley, D. G.; Skelly, P. J.; Tighe, B. J. *Br. Polym. J.* **1980**, *12*, 99.
(14) Leach, J. B.; Bivens, K. A.; Patrick, C. W., Jr.; Schmidt, C. E. *Biotechnol. Bioeng.* **2003**, *82*, 578.
(15) Luo, Y.; Kirker, K. R. Prestwich, G. D. Modification of Natural Polymers: Hyaluronic Acid. In Atala, A., Lanza, R., Eds.; *Methods of Tissue Engineering*; Academic Press: San Diego, 2001; pp 539−553.
(16) Bouhadir, K. H.; Hausman, D. S.; Mooney, D. J. *Polymer* **1999**, *40*, 3575.
(17) Okano, T.; Katayama, M.; Shinohara, I. *J. Appl. Polym. Sci.* **1978**, *22*, 369.
(18) Lu, Z.-R.; Kopečková, P.; Wu, Z.; Kopečková, J. *Bioconjugate Chem.* **1999**, *9*, 793.
(19) Okano, T.; Katayama, M.; Shinohara, I. *J. Appl. Polym. Sci.* **1978**, *22*, 369.
(20) Bulpitt, P.; Aeschlimann, D. *J. Biomed. Mater. Res.* **1999**, *47*, 152.
(21) Weissmann, B. *J. Biol. Chem.* **1955**, *216*, 783.
(22) Gilbert, B. C.; King, D. M.; Thomas, C. B. *Carbohydr. Res.* **1984**, *125*, 217.
(23) Barbucci, R.; Lamponi, S.; Borzacchiello, A.; Ambrosio, L.; Fini, M.; Torricelli, P.; Giardino, R. *Biomaterials* **2002**, *23*, 4503.
(24) Kong, H. J.; Wong, E.; Mooney, D. J. *Macromolecules* **2003**, *36*, 4582.
(25) Rosowski, J. J.; Brinsko, K. M.; Tempel, B. L.; Kujawa, S. G. *J. Assoc. Res. Otolaryngol.* **2003**, *4*, 371.
(26) Rosowski, J. J.; Mehta, R. P.; Merchant, S. N. *Otol. Neurotol.* **2003**, *24*, 165.
(27) Ferry, J. D. *Viscoelastic Properties of Polymers*, 3rd ed.; Wiley: New York, 1980.
(28) Bird, R. B.; Armstrong, R. C.; Hassager, O. *Dynamics of Polymeric Liquids*; Wiley: New York, 1977; Vol. 1, pp 129−204, 275−303.
(29) Chan, R. W.; Titze, I. R. *J. Acoust. Soc. Am.* **1999**, *106*, 2008.
(30) Bryant, S. J.; Nuttelman, C. R.; Anseth, K. S. *J. Biomater. Sci., Polym. Ed.* **2000**, *11*, 439.
(31) Carrier, G. F.; Krook, M.; Pearson, C. E. *Functions of a Complex Variable*; McGraw-Hill: New York, 1996.
(32) Pipkin, A. C. *Lectures on Viscoelasticity Theory*; Springer-Verlag: New York, 1972.
(33) Schapery, R. A. A Theory of Non-Linear Thermoviscoelasticity Based on Irreversible Thermodynamics. *Proc. Fifth U.S. Natl. Congr. Appl. Mech., ASME* **1966**, 511−530.

MA035970W